Materials Research. 2019; 22(2): e20180493
DOI: http://dx.doi.org/10.1590/1980-5373-MR-2018-0493

Investigation on Structural, Morphological and Relaxometric Properties of Lamellar Zrp Modified with Long Chain Amine

Danielle de Mattos Mariano[a], Daniela de França da Silva Freitas[a], Luis Claudio Mendes[a]*, Ana Luiza Fonseca Carvalho[a], Flavio James Humberto Tommasini Vieira Ramos[b]

[a]Universidade Federal do Rio de Janeiro - UFRJ, Instituto de Macromoléculas Professora Eloisa Mano - IMA, Avenida Horácio Macedo, 2030, Centro de Tecnologia, Bloco J, 21941-598, Ilha do Fundão, Rio de Janeiro, RJ, Brasil
[b]Instituto Militar de Engenharia - IME, Praça General Tibúrcio, 80, 22290-270, Urca, Rio de Janeiro, RJ, Brasil

Received: July 11, 2018; Revised: October 19, 2018; Accepted: December 03, 2018

In order to search nanofiller for controlling release of drugs lamellar α-zirconium phosphate (α-ZrP) was modified with ether-amine oligomer (E-A). Synthesis and chemical modification followed specific reaction conditions and different EA:ZrP ratios. Infrared spectra showed strong interaction between P-OH and NH_2 groups. Thermogravimetric curves showed that ether-amine oligomer was incorporated by ZrP. Interlamellar space of α-ZrP increased at least four times indicating intercalation. The relaxometry analysis indicated that α-ZrP molecular mobility changed according to the ether-amine amount. The scanning electron microscopy/energy dispersive analysis revealed the presence of octadecylamine inside the α-ZrP galleries. The results showed that P-OH group (Brønsted acid) and amine group (Brønsted base) reacted to each other, resulting in an ionic bond $PO^{-}{}_{3}HN^{+}$-[-(CH_2-CH_2-O)$_m$-(CH_2-C-H(CH_3)-O)$_n$-]. Partially intercalated nanofiller were achieved.

Keywords: *Ether-amine, intercalation, organomodification, zirconium phosphate.*

1. Introduction

Inorganic layered nanomaterials have been investigated for wide range of applications such as control drug release and reinforcing filler in nanocomposites. Inorganic lamellar phosphates have been gaining remarkable interest as alternative for natural clays in some many kind of applications. Nanospheres of titanium phosphate functionalized by metal ion were developed by Feng *et al.* for detection of myocardial infraction[1]. Chenlu *et al.* dispersed nanosheets of titanium phosphate in poly(vinyl alcohol) (PVA) owing to obtaining nanocomposite. The authors reported that marked enhance of properties was achieved[2]. Rathore and Pathania carried out the degradation of methylene blue in presence of photocatalyst based on styrene-tin phosphate ion exchanger. They mentioned an efficiency of 80% after two hours of solar light exposure[3]. Synthetic phosphates have been studied since 60's. They presented generic chemical formula $M(RPO_3)_2$ where M is a tetravalent metal for instance, titanium (Ti), zirconium (Zr), hafnium (Hf), germanium (Ge), tin (Sn), plumb (Pb), torium (Th) and R can be hydrogen atom, hydroxyl group or an organic moiety[4,5]. There are several articles devoted to the synthesis of lamellar zirconium phosphate (α-ZrP) and zirconium compounds for application in polymer nanocomposites and so on[6-13]. Due to their crystalline lamellar structure and the presence of acid groups inside the galleries, they allow the anchoring of intercalant in order to expand their lamellae.

Short and long chain amines have been used as intercalation agent. Alhendawi *et al.* investigated the intercalation of a series of primary alkylamines of different chain length inside the galleries of λ-ZrP[14]. Aminoalkanes were intercalated into λ-ZrP to use as latent polymerization catalyst of glycidyl phenyl ether (GPE)[15]. The intercalation of n-alkylamines (n-butylamine, n-heptylamine and n-decylamine) into layered zirconium benzylamino-N,N-dimethylphosphonate phosphate (ZBMPA) ZBMPA was reported by Zeng *et al.*[16].

Oligo-ether-amine (*Jeffamine*) is a commercial class of amines with great application. White *et al.* reported the influence of oligo-ether-amine (M-600 and M-1000) as surface modifiers on the rheology of epoxy/ZrP suspensions[17]. ZrP nanoplatelets were organically modified with oligo-ether-amine M-1000 in order to obtain α-zirconium phosphate/polyurethane (ZrP/PU) nanocomposites for corrosion protection[18]. kłapyta *et al.*[19] inserted monoamines (*Jeffamines* M-600, M-1000 and M-2005) into a synthetic Li-fluorotaeniolite (Li-TN). The authors pointed out that the Li-TN was also easily intercalated with the unprotonated *Jeffamines* in a water-ethanol solution. Sue *et al*.[20] studied the fracture behaviour of epoxy nanocomposites containing α-zirconium phosphate modified with monoamine (*Jeffamine* 715). It was not found article exclusively devoted to the systematic study of intercalation of α-ZrP using ether-amine oligomer (*Jeffamine* M600). Searching nanofiller for controlling release of drugs α-ZrP

*e-mail: lcmendes@ima.ufrj.br

was modified with ether-amine oligomer (E-A, *Jeffamine* M-600) Three ether-amine:ZrP molar ratios (0.5:1, 1:1 and 2:1) were investigated. The investigation on structural, thermal, crystallographic and morphological characteristics was evaluated.

The aim of this work was to prepare organointercalated zirconium phosphate and to evaluate the effect of different ether-amine:phosphate ratio on thermal, structural, crystallographic and molecular mobility characteristics of the filler. The insertion of the E-A in ZrP had showing marked changes on the relaxation times, degree of crystallinity and thermal stability. In the future, the nanofiller will be used to produce nanocomposite viewing controlling release of drugs.

2. Materials and Methods

2.1. Materials

Phosphoric acid (H_3PO_4), zirconium (IV) oxide chloride 8-hydrate ($ZrOCl_2.8H_2O$), ethyl alcohol and ether-amine (*Jeffamine*® M-600, 600 g/mol) were obtained by Sigma-Aldrich Co. Herein, the *Jeffamine* was named as ether-amine oligomer and abbreviated as E-A.

2.2 Methods

2.2.1 Synthesis of layered zirconium phosphate

The synthesis of lamellar-zirconium phosphate was performed by direct precipitation. 12M phosphoric acid solution and zirconium oxychloride at a ratio Zr/P = 18 were mixed, kept under reflux at 110°C, under stirring, during 24 hours. The product was centrifuged and solid portion was washed successively until pH around 5. Finally, the lamellar zirconium phosphate was lyophilized[21-22]. The amorphous structure of ZrP is achieved by of reaction of zirconium oxychloride ($ZrOCl_2.8H_2O$) in excess phosphoric acid, according to equation (Equation 1):

$$ZrOCl_2.8H_2O + 2H_3PO_4 \rightarrow Zr(HPO_4)_2.H_2O + 2HCL + 8H_2O \quad (1)$$

2.2.2. Jeffamine (M600) intercalation in zirconium phosphate

The chemical modification of the lamellar zirconium phosphate was carried out through the addition of ether-amine oligomer at different ether-amine/phosphate ratios (0.5:1; 1:1; 2:1). Ethanolic solution of lamellar zirconium phosphate was added to the ether-amine ethanolic solution being the reaction medium maintained at 25°C, under stirring, during 24 hours. The product was dried at 110°C until constant weight was attained[23].

2.3. Characterizations

2.3.1. Infrared spectroscopy (FTIR)

Infrared spectroscopy was performed in Perkin Elmer equipment, model Frontier. The spectrum was taken by KBr disk, in the range of 4000-400 cm^{-1} with 50 scans and 4 cm^{-1} of resolution. The effect of the ether-amine oligomer amount on the P-OH group was carried out considering the determination of ratio among the variable bands at 3,595; 3,511 and 3,153 cm^{-1} and invariable one at 2,972 cm^{-1}. Also, the ratio between bands at 1,617 cm^{-1} and 2,972 cm^{-1} was assessed in order to discuss on the amount of water remained in the modifier ZrP.

2.3.2. Wide-angle X-ray diffraction (WAXD)

WAXD was performed using Rigaku equipment, model Ultima IV, CuKα radiation with wavelength (1.5418 Å) Ni filter, 30 kV voltage and current of 15 mA, 2θ between 2-50° and resolution of 0,05º. With and without modification, the interlayer spacing of zirconium phosphate was evaluated by Bragg equation (Equation 2):

$$n = 2d_{hkl}\,\mathrm{sen}\theta \quad (2)$$

n - diffraction order;
d_{hkl} - interlayer spacing;
θ - diffraction angle.

2.3.3. Thermogravimetry (TG/DTG)

Thermal stability was evaluated using a thermogravimetric analyser, TA Instrument, model Q500. The analysis was carried out from 30 to 700°C, at 10°C/min, with nitrogen as carrying gas. Degradation temperatures - Onset, maximum and final, respectively, T_{onset}, T_{max} and T_{final} were registered.

2.3.4. Differential scanning calorimetry (DSC)

Calorimetric analysis was carried out using TA Instruments, model Q1000. Three thermal cycles were performed. Firstly, the sample was heated from - 30 to 200°C, 10°C/min, under nitrogen atmosphere, maintained at this temperature for 2 minutes, in order to eliminate the thermal history. After that, a cooling cycle was carried out until - 30°C, at 10°C/min. Finally, a second heating was conducted in the same conditions of the initial cycle.

2.3.5. Hydrogen low-field nuclear magnetic resonance (LFNMR)

In order to assess the molecular mobility, the polymer relaxation time was investigated using ^{1}H low-field nuclear magnetic resonance (^{1}HLFNMR) analysis. It was performed in

a Maran Ultra 23 low-field NMR device. The relaxation time (T_1H) was measured in time intervals of 2 s and 40 points, at 30°C. The result was expressed in terms of domain curves.

2.3.6. Scanning Electron Microscopy (SEM) and X-ray scatteringspectrometer (EDX)

Scanning electron microscopy (SEM) was performed with FEG Quanta 250 microscope using sample fractured surface covered with gold and applying voltage of 30 kV. Photographs were taken at high magnification. For the elements identification, an X-ray analyzer BRUKER was coupled to the SEM.

3. Results and Discussion

3.1. Infrared spectroscopy (FTIR)

Figure 1 (a) shows FTIR spectra of the ether-amine oligomer, α-ZrP and modified ZrP with different E-A:ZrP ratios. For ether-amine oligomer, absorption bands at 2,972, 2,931 and 2,873 cm^{-1}; l,460 cm^{-1}; 1,108 and 1,016 cm^{-1}; were respectively assigned as CH stretching, CH_2 stretching and C-O-C stretching of ethylene and propylene oxide chain moieties[24]. For ZrP, absorption bands at 3,595, 3,511 and 3,153 cm^{-1} were attributed to the asymmetric/ symmetric stretching of the crystal/interlayer water and hydrogen bonding between H-O-H and P-OH group[25]. Absorption bands around 1,112; 1,074; 1,050; 980 and 968 cm^{-1} were concerned to the phosphate asymmetric and symmetric vibrations[26-27]. Similarities were noticed for all modified α-ZrP. Absorption bands at 3,595; 3,511cm^{-1}; 3,153 remained but the intensity was lower for sample 2:1 E-A/ZrP ratio. The ether-amine oligomer absorption bands at 2,972; 2,931 and 2,873 cm^{-1} appeared. Infrared absorptions at 1,112; 1,074; 1,050; 980 and 968 cm^{-1} assigned as vibrations of PO_4^{3-} were shifted to lower wavenumbers[27]. The same has occurred for ether-amine oligomer absorption bands at 1,108 and 1,016 cm^{-1} but both were superimposed by α-ZrP ones. In this work, the P-OH group was considered as Brønsted acid while the NH_2 group was seen as Brønsted base. Figure 1

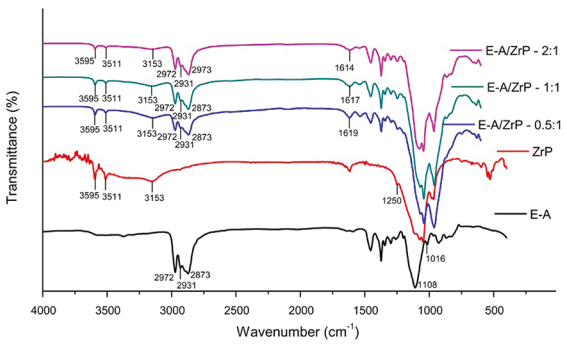

(a)

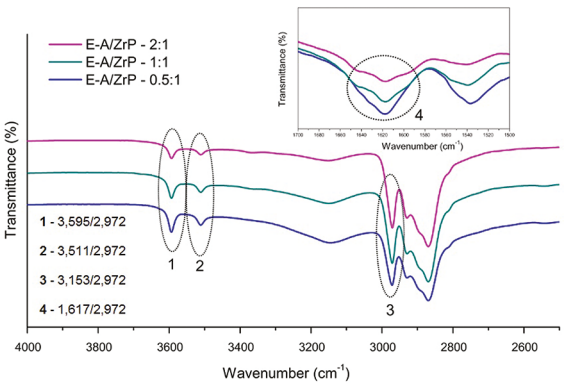

(b)

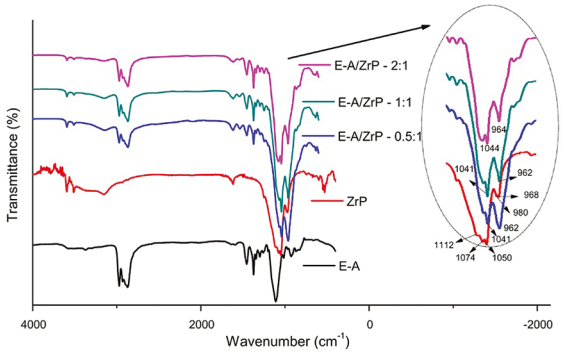

(c)

Figure 1. (a) FTIR spectra of the ether-amine oligomer, ZrP and modified ZrP, (b) FTIR spectra of the modified phosphates indicating changes in band shapes, and (c) Highlighted crystal/interlayer water absorption bands.

(b) highlights the variable bands at 3,595; 3,511, 3,153 and 1,617 cm^{-1}. These bands were related with the invariable one at 2,972 cm^{-1} in order to estimate the reaction degree between P-OH and NH_2 groups. Table 1 shows the variation of these band ratio according to the nanofiller. The ratios decreased indicating that the groups reacted to each other resulting an ionic bond $PO^{-}{}_{3}HN$-[-(CH_2-CH_2-O)$_m$-(CH_2-C-H(CH_3)-O)$_n$-]. Changed of the outline of the spectra between 1,200-900 cm^{-1} (Figure 1 c) corroborated the occurrence of Brønsted acid-base reaction between P-OH and amine groups[28].

3.2. Wide-angle X-ray diffraction (WAXD)

Figure 2 (a) shows WAXD patterns of the samples. The diffractogram of the α-ZrP showed characteristic diffraction angles around 2θ = 11.75°, 19.89° and 25.04° and lamellar $d_{spacing}$ of 7.52 Å similarly to reported by Brandão *et al*., Hajipour *et al*. and Thakur *et al*. [9,27,29]. The ether-amine oligomer showed diffraction pattern of amorphous material. The $d_{spacing}$ for each modified α-ZrP is shown in Table 2. For all modified α-ZrP, the original *hkl* 002 remained with less intensity but a series of new angles below 2θ = 10° indicated that the original α-ZrP structure was partially destroyed. To these low angles the $d_{spacing}$ increased as diffraction angle decreased. The $d_{spacing}$ attained value almost four times higher than α-ZrP precursor. The larger interlayer spacing was attributed to the entrance of ether-amine oligomer into the α-ZrP nanoplatelets. Similar result was reported by Sun *et al.* in their investigation about ZrP crystallinity and its effect on monoamine intercalation[30]. Partial intercalation was attained and schematic representation of amine arrangement inside of the α-ZrP is shown in Figure 2 (b).

Table 1. Band ratios as function of E-A oligomer content.

Sample	Band ratio			
	3,595 / 2,972	3,511 / 2,972	3,153 / 2,972	1,617 / 2,972
E-A/ZrP – 0.5:1	0.32	0.23	0.44	0,28
E-A/ZrP – 1:1	0.26	0.19	0.30	0,19
E-A/ZrP – 2:1	0.18	0.15	0.21	0.13

3.3. Thermogravimetry (TG/DTG)

Figures 3 show thermogravimetric/thermogravimetric derivative curves. Thermal properties, theoretical/experimental E-A/ZrP ratios and chemical formula of α-ZrP precursor and modified are arranged in Table 3. Theoretical and experimental E-A/ZrP ratios were very similar showing that the effectiveness of intercalation. α-ZrP showed three degradation steps.

Table 2. Diffraction angles and dspacing of modified zirconium phosphate at different E-A/ZrP ratios.

E-A/ZrP – 0.5:1		E-A/ZrP – 1:1		E-A/ZrP – 2:1	
3.15 °	28.02 Å	3.10 °	28.48 Å	3.10 °	28.48 Å
4.70°	18.79 Å	4.55°	19.40 Å	4.70°	18.79 Å
11.65°	7.59 Å	6.10°	14.48 Å	6.10°	14.48 Å
		7.60°	11.62 Å	7.75°	11.40 Å
		9.10°	9.71 Å	11.55°	7.65 Å
		11.70°	7.56 Å		

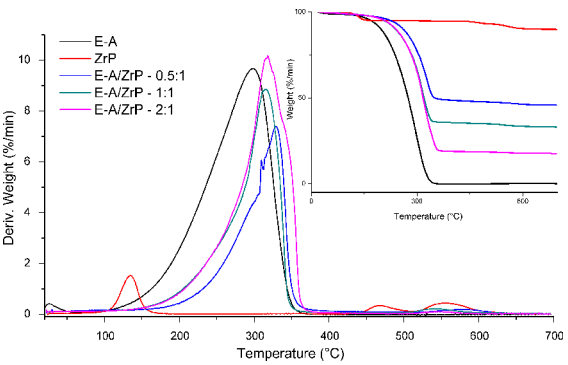

Figure 3. TG and DTG curves of the ZrP and modified zirconium phosphates.

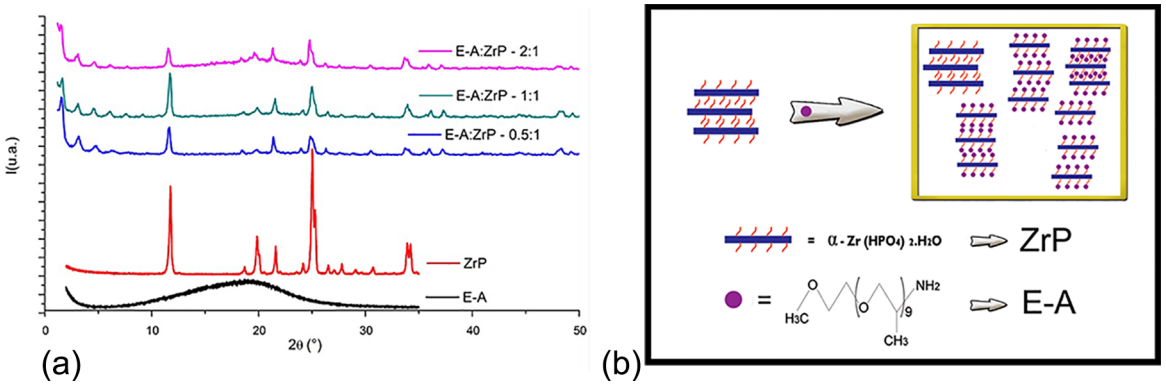

Figure 2. (a) WAXD diffractograms of the ZrP and modified zirconium phosphates, and (b) Schematic representation of the E-A oligomer insertion into ZrP galleries.

Table 3. TG/DTG data of the ZrP and modified zirconium phosphates.

Sample	Formula obtained	A*	B*	T_{onset}/°C	T_{max}/°C	T_{max}/°C	T_{max}/°C
E-A		---	---	225	299	---	---
ZrP	$Zr(HPO_4)_2 0.658H_20$	---	---	118	135	466	555
E-A/ZrP – 0.5:1	$Zr(HPO_4)_2(E\text{-}A)_{0.48}.0.5689H_2O$	0.5:1	0.48	276	329	577	---
E-A/ZrP – 1:1	$Zr(HPO_4)_2(E\text{-}A)_{0.84}.0.7544H_2O$	1:1	0.84	264	315	541	---
E-A/ZrP – 2:1	$Zr(HPO_4)_2(E\text{-}A)_{1.92}.1.2632H_2O$	2:1	1.92	269	318	---	---

*A -Theoretical amine/phosphate ratio;

*B -Experimental amine/phosphate ratio

The first around 100-200°C, the second at 400-500°C and third in the vicinity of 500-600°C were associated to the releasing of adsorbed water, α-ZrP dehydroxylation and chemical transformation from phosphate to pyrophosphate, respectively[23]. The amine initiated its degradation at 225°C and T_{max} occurred at 299°C. Dal pont *et al.* proposed the existence of different degradation steps for weakly linked amine and strongly linked amine in ZrP intercalation[6]. This was not observed in our investigation. Modified nanofillers presented three steps of degradation. The degradation below 300°C was attributed to the releasing of free amine while that nearby 300-350°C was associated to the bonded amine as seen in the ionic bond $PO^{-+}{}_3HN$-[-$(CH_2$-CH_2-O$)_m$-$(CH_2$-C-H(CH_3)-O$)_n$-]. The final degradation step was associated to the conversion of phosphate to pyrophosphate. Our results are in agreement with reported by Bestaoui *et al.*[24].

3.4. Differential scanning calorimetry (DSC)

In order to normalize this evaluation, it was considered the thermal events occurred at second heating cycle (Figure 4). As shown by the calorimetric curves, either zirconium phosphate or ether-amine did not show relaxation in the temperature range. Similar results were presented by samples E-A/ZrP (0.5:1 and 1:1). Only thermal curve of E-A/ZrP (2:1) sample showed an endothermic peak around 100°C which was attributed to the adsorbed water similarly to reported by Mendes *et al.*[23].

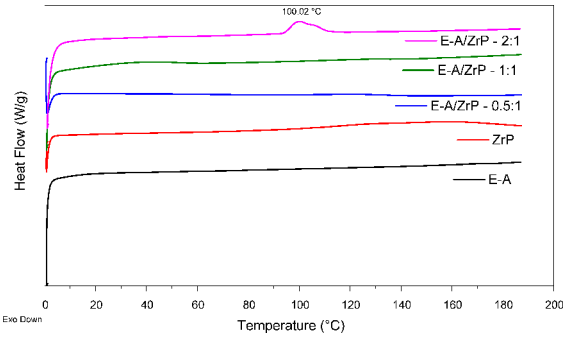

Figure 4. DSC second heating curves of the ZrP and modified zirconium phosphates.

3.5. Hydrogen low-field nuclear magnetic resonance (^{1}HLFNMR)

The effect of inorganic fillers on the molecular mobility of polymer matrix through hydrogen low-field nuclear magnetic resonance (^{1}HLFNMR) has been studied[31-34]. Herein, this technique was applied in order to evaluate the action of amine on the α-ZrP relaxometry. Figure 5 and Table 4 show the domain curves and relaxation times of precursor α-ZrP and modified ones, respectively. The precursor α-ZrP curve presented a bimodal relaxation peak in the time intervals of $8x10^4$-$4x10^5$ ms (peak 1) and $4x10^5$-$3x10^6$ ms (peak 2). It was deduced that the peak 1 represents hydrogen relaxation of P-OH group bonded with water while the peak 2 is concerned

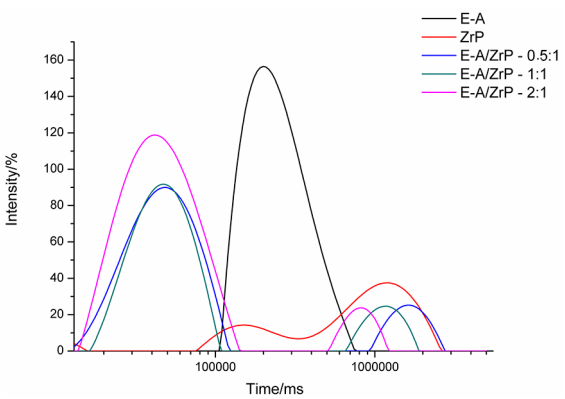

Figure 5. Domain curves of the ZrP and modified phosphates.

Table 4. T1H of the ZrP and modified phosphates.

Samples	T_1H (ms)	T_1H (ms)
E-A	238	---
ZrP	133	816
E-A/ZrP – 0.5:1	48	943
E-A/ZrP – 1:1	48	758
E-A/ZrP – 2:1	41	656

to the hydrogen relaxation of free P-OH. The amine showed one peak between 10^5-10^6 ms. Similarly, the modified α-ZrP also presented two relaxation peaks. For any E-A:ZrP ratios, the first peak was in the time interval around $1x10^4$-$1x10^5$ ms. This peaks was slightly displaced to lower values compared to that of precursor α-ZrP. According to the E-A:ZrP ratio, the second peak showed tendency to shift along the time axis. From smallest to highest amine content, the values were around $9x10^5$-$3x10^6$, $7x10^5$-$2x10^6$ and $5x10^5$-$1x10^6$ ms, respectively. In general, as can be seen in Table 4, there was a reduction of the α-ZrP relaxation times as the amine content increased. In this study, it was proposed the occurence of reaction between P-OH (Brønsted acid) and amine group (Brønsted base). The insertion of amine into α-ZrP platelets created an ionic bond $PO^{-}{}_3HN$-[-$(CH_2$-CH_2-$O)_m$-$(CH_2$-C-$H(CH_3)$-$O)_n$-] reduced the its packing favoring the enhance of molecular mobility.

3.6. Scanning Electron Microscopy (SEM) and X-ray scattering spectrometer (EDX)

The representative SEM image of α-ZrP is shown in Figure 6 a-b. The nanofiller presented as agglomerate of nanoplates with pseudo-hexagonal shape similarly to found by Xia *et al.* and Yue *et al.* in their articles on intercalation the α-ZrP with ionic liquids and benzoxazine, respectively[35-36]. A representative SEM image of E-A/ZrP is located at Figure 6 d-e. Where it was possible and just to have an idea about the thickness, some nanoplates showed thickness about 200 nm and diameter around 300 nm. The presence of amine disturbed the original arrangement of the filler. It is possible to see that the amine is structured among the ZrP interlayers suggesting pillarization (Figure 6 e). Figure 6 c-f shows the EDX spectra of α-ZrP and E-A/ZrP. It revealed the presence of O, P and Zr as the main elements of ZrP (Figure 6 c). Similar result was found by Wu *et al.* and Yu *et al.*[37-38]. The EDX spectrum of E-A/ZrP (Figure 6 f) revealed elements such as C, O, N, P and Zr. Due to the incorporation of the amine in the galleries of the zirconium phosphate, it was observed the variation of zirconium and oxygen content in E-A/ZrP sample. Similar result was found by Khare and Chokhare[39] in their work on Fe(Salen) intercalated α-zirconium phosphate for the oxidation of cyclohexene.

4. Conclusions

It was studied the intercalation long chain amine at different molar ratios (0.5:1, 1:1, and 2:1) into interlayer space of lamellar a-ZrP. Thermogravimetric and relaxometric results were influenced by amine:phosphate ratio. It was attained significant increasing of $d_{spacing}$. Infrared analysis indicated that Brønsted acid-base reaction between P-OH (Brønsted acid) and amine (Brønsted base) occurred. The SEM/EDX revealed pseudo-hexagonal shape and the entrance of amine inside the a-ZrP galleries.

5. Acknowledgements

The authors thank the Conselho Nacional de Desenvolvimento Científico e Tecnológico (CNPq), Coordenação de Aperfeiçoamento de Pessoal de Nível Superior (CAPES)

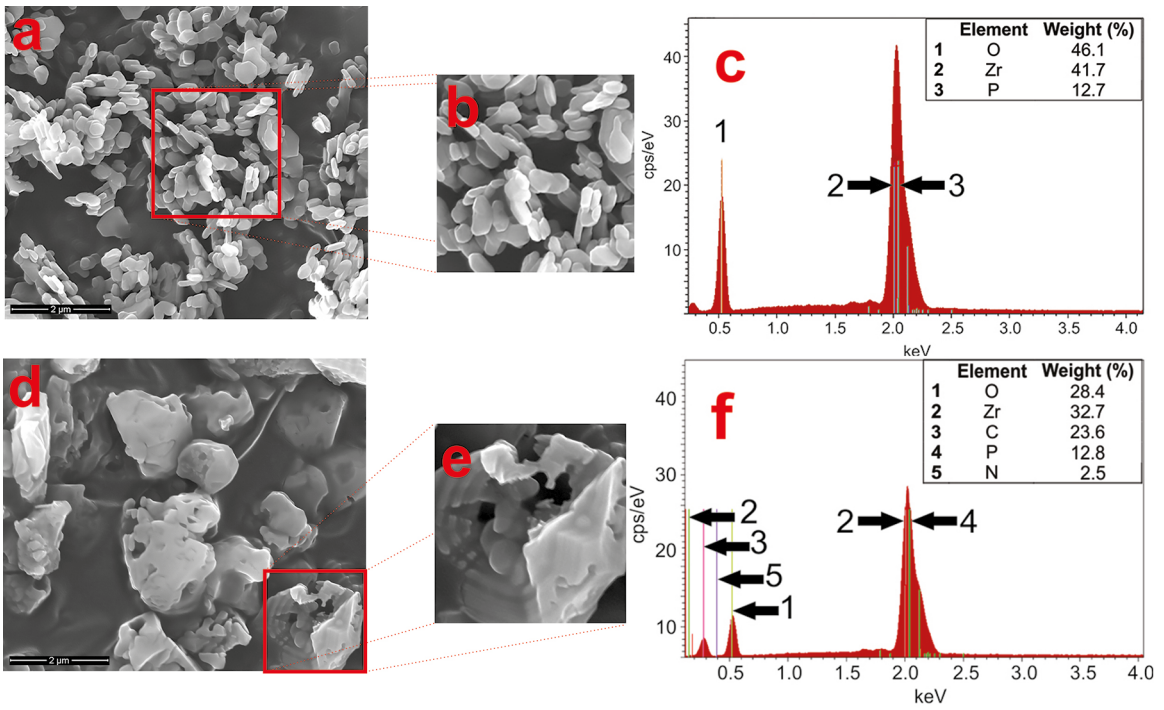

Figure 6. (a) and (d) EDX spectra of ZrP and E-A/ZrP; (b), (c), (e) and (f) SEM micrographs of ZrP and E-A/ZrP.

and the staff of Universidade Federal do Rio de Janeiro for supporting this work.

6. References

1. Feng LN, Bian ZP, Peng J, Jiang F, Yang GH, Zhu YD, et al. Ultrasensitive Multianalyte Electrochemical Immunoassay Based on Metal Ion Functionalized Titanium Phosphate Nanospheres. Analytical Chemistry. 2012;84(18):7810-7815.

2. Bao C, Guo Y, Song L, Lu H, Yuan B, Hu Y. Facile Synthesis of Poly(vinyl alcohol)/a-Titanium Phosphate Nanocomposite with Markedly Enhanced Properties. I&EC Research. Industrial & Engineering Chemistry Research. 2011;50(19):11109-11116.

3. Rathore BS, Pathania D. Styrene-tin (IV) phosphate nanocomposite for photocatalytic degradation of organic dye in presence of visible light. Journal of Alloys and Compounds. 2014;606:105-111.

4. Plundrich GT, Wadepohl H, Gade LH. Synthesis and Reactivity of Group 4 Metal Benzyl Complexes Supported by Carbazolide-Based PNP Pincer Ligands. Inorganic Chemistry. 2016;55(1):353-365.

5. Alberti G, Costantino U, Allulli S, Tomassini N. Crystalline Zr(R-PO3)2 and Zr(R-OPO3)2 compounds (R=organic radical): A new class of materials having layered structure of the zirconium phosphate type. Journal of Inorganic and Nuclear Chemistry. 1978;40(6):1113-1117.

6. Dal pont K, Gérard JF, Espuche E. Modification of a-ZrP nanofillers by amines of different chain length: Consequences on the morphology and mechanical properties of styrene butadiene rubber based nanocomposites. European Polymer Journal. 2012;48(1):217-227.

7. Ma J, Liu C, Li R, Wu H, Zhu L, Yang Y. Preparation and properties of castor oil-based polyurethane/a-zirconium phosphate composite films. Journal of Applied Polymer Science. 2011;121(3):1815-1822.

8. Wang DY, Liu XQ, Wang JS, Wang YZ, Stec AA, Hull TR. Preparation and characterization of a novel fire retardant PET/a-zirconium phosphate nanocomposite. Polymer Degradation and Stability. 2009;94(4):544-549.

9. Brandão LS, Mendes LC, Medeiros ME, Sirelli L, Dias ML. Thermal and mechanical properties of poly(ethylene terephthalate)/lamellar zirconium phosphate nanocomposites. Journal of Applied Polymer Science. 2006;102(4):3868-3876.

10. Thakur VK, Li Y, Wu H, Kessler MR. Synthesis, characterization, and functionalization of zirconium tungstate (ZrW2O8) nano-rods for advanced polymer nanocomposites. Polymers for Advanced Technologies. 2017;28(11):1375-1381.

11. Lino AS, Mendes LC, Silva DF, Malm O. High density polyethylene and zirconium phosphate nanocomposites. Polímeros. 2015;25(5):477-482.

12. Freitas DFS, Mendes LC, Lino AS. Polyamide-6/Organointercalated Lamellar Zirconium Phosphate Nanocomposites: Molecular Mobility, Crystallography and Thermo-Mechanical Evaluation. Journal of Nanoscience and Nanotechnology. 2017;17(5):3042-3050.

13. Carvalho ALF, Freitas DFS, Mariano DM, Mattos GC, Mendes LC. Influence of zinc gluconate as intercalating agent on the structural, thermal, morphologic, and molecular mobility of lamellar nanofiller. Colloid and Polymer Science. 2018;296(6):1079-1086.

14. Alhendawi H, Brunet E, Hammouda H, Payán ER, Juanes O. Intercalation of primary alkylamines into lambda-zirconium phosphate: lambda-type materials with extended interlayer separation. Journal of Porous Materials. 2016;23(6):1519-1526.

15. Shimomura O, Maeno K, Ohtaka A, Yamaguchi S, Ichihara J, Sakamoto K, et al. Alkylamines-intercalated a-zirconium phosphate as latent thermal anionic initiators. Journal of Polymer Science Part A: Polymer Chemistry. 2014;52(13):1854-1861.

16. Zeng R, Fu X, Sui Y, Yang X, Sun M, Chen J. Synthesis, characterization and intercalation property of layered zirconium benzylamino-N,N-dimethylphosphonate phosphate materials. Journal of Organometallic Chemistry. 2008;693(16):2666-2672.

17. White KL, Li P, Yao H, Nishimura R, Sue HJ. Effect of surface modifier on flow properties of epoxy suspensions containing model plate-like nanoparticles. Rheologica Acta. 2014;53(7):571-583.

18. Huang TC, Lai GH, Li CE, Tsai MH, Wan PY, Chung YH, et al. Advanced anti-corrosion coatings prepared from a-zirconium phosphate/polyurethane nanocomposites. RSC Advances. 2017;7(16):9908-9913.

19. Klapyta Z, Gawel A, Fujita T, Iyi N. Intercalation of protonated polyoxyalkylene monoamines into a synthetic Li-fluorotaeniolite. Applied Clay Science. 2011;52(1-2):133-139.

20. Sue HJ, Gam KT, Bestaoui N, Clearfield A, Miyamoto M, Miyatake N. Fracture behavior of a-zirconium phosphate-based epoxy nanocomposites. Acta Materialia. 2004;52(8):2239-2250.

21. Alberti G. Syntheses, crystalline structure, and ion-exchange properties of insoluble acid salts of tetravalent metals and their salt forms. Accounts of Chemical Research. 1978;11(4):163-170.

22. Mendes LC, Silva DF, Lino AS. Linear low-density polyethylene and zirconium phosphate nanocomposites: evidence from thermal, thermo-mechanical, morphological and low-field nuclear magnetic resonance techniques. Journal of Nanoscience and Nanotechnology. 2012;12(12):8867-8873.

23. Mendes LC, Silva DF, Araujo LJF, Lino AS. Zirconium phosphate organically intercalated/exfoliated with long chain amine. Journal of Thermal Analysis and Calorimetry. 2014;118(3):1461-1469.

24. Bestaoui N, Spurr NA, Clearfield A. Intercalation of polyether amines into a-zirconium phosphate. Journal of Materials Chemistry. 2006;16(8):759-764.

25. Díaz A, Mosby BM, Bakhmutov VI, Martí AA, Batteas JD, Clearfield A. Self-Assembled Monolayers Based Upon a Zirconium Phosphate Platform. Chemistry of Materials. 2013;25(5):723-728.

26. Wei S, Lizu M, Zhang X, Sampathi J, Sun L, Milner MF. Electrospun poly(vinyl alcohol)/a-zirconium phosphate nanocomposite fibers. High Performance Polymers. 2013;25(1):25-32.

27. Hajipour AR, Karimi H. Synthesis and characterization of hexagonal zirconium phosphate nanoparticles. Materials Letters. 2014;116:356-358.

28. Thakur VK, Vennerberg D, Kessler MR. Green Aqueous Surface Modification of Polypropylene for Novel Polymer Nanocomposites. ACS Applied Materials & Interfaces. 2014;6(12):9349-9356.

29. Thakur VK, Yan J, Lin MF, Zhi C, Golberg D, Bando Y, et al. Novel polymer nanocomposites from bioinspired green aqueous functionalization of BNNTs. Polymer Chemistry. 2012;3(4):962-969.

30. Sun L, Boo WJ, Browning RL, Sue HJ, Clearfield A. Effect of Crystallinity on the Intercalation of Monoamine in a-Zirconium Phosphate Layer Structure. Chemistry of Materials. 2005;17(23):5606-5609.

31. Villaça JC, da Silva LCRP, de Alexandria AK, de Almeida GS, Locatelli FR, Maia LC, et al. Development and characterization of clay-polymer nanocomposite membranes containing sodium alendronate with osteogenic activity. Applied Clay Science. 2017;146:475-486.

32. da Silva PSR, Iulianelli GCV, Tavares MIB. Spin-Spin Relaxation Time to Evaluate Degradation of HIPS/Organoclaynano Composites by Aging. Materials Sciences and Applications. 2017;8(5):76421.

33. Chimanowsky Junior JP, Dutra Filho JC, Tavares MIB. Nuclear magnetic resonance as a powerful tool for evaluation of intermolecular interaction: Correlation with rheological measurements of recycled nanocomposite. Polymer Testing. 2017;63:417-426.

34. Silva MBR, Tavares MIB, Marsaro Junior AW, Cucinelli Neto RP. Evaluation of Intermolecular Interactions in the PHB/ZnO Nanostructured Materials. Journal of Nanoscience and Nanotechnology. 2016;16(7):7606-7610.

35. Xia F, Yong H, Han X, Sun D. Small Molecule-Assisted Exfoliation of Layered Zirconium Phosphate Nanoplatelets by Ionic Liquids. Nanoscale Research Letters. 2016;11:348.

36. Yue J, Zhao C, Dai Y, Hui L, Li Y. Catalytic effect of exfoliated zirconium phosphate on the curing behavior of benzoxazine. Thermochimica Acta. 2017;650:18-25.

37. Wu Z, Zhang L, Guan Q, Ning P, Ye D. Preparation of a-zirconium phosphate-pillared reduced graphene oxide with increased adsorption towards methylene blue. Chemical Engineering Journal. 2014;258:77-84.

38. Yu S, Gao X, Jing H, Zhang R, Gao X, Su H. Fabrication and characterization of novel magnetic/luminescent multifunctional nanocomposites for controlled drug release. CrystEngComm. 2014;16(29):6645-6653.

39. Khare S, Chokhare R. Synthesis, characterization and catalytic activity of Fe(Salen) intercalated a-zirconium phosphate for the oxidation of cyclohexene. Journal of Molecular Catalysis A: Chemical. 2011;344(1-2):83-92.